Remote Sensing of Environment 142 (2014) 69–82

Contents lists available at ScienceDirect

Remote Sensing of Environment

journal homepage: www.elsevier.com/locate/rse

# Enhanced landslide investigations through advanced DInSAR techniques: The Ivancich case study, Assisi, Italy ☆

Fabiana Calò [a], Francesca Ardizzone [b], Raffaele Castaldo [a,b], Piernicola Lollino [c], Pietro Tizzani [a], Fausto Guzzetti [b], Riccardo Lanari [a], Maceo-Giovanni Angeli [b], Fabrizio Pontoni [d], Michele Manunta [a,*]

[a] CNR IREA, via Diocleziano 328, 80124 Napoli, Italy
[b] CNR IRPI, via della Madonna Alta 126, 06128 Perugia, Italy
[c] CNR IRPI, via Amendola 122 I, 70126 Bari, Italy
[d] Geoequipe, via Sandro Pertini, 62029 Tolentino, Italy

ARTICLE INFO

*Article history:*
Received 19 May 2013
Received in revised form 17 October 2013
Accepted 5 November 2013
Available online 10 December 2013

*Keywords:*
Synthetic aperture radar (SAR)
Differential SAR interferometry (DInSAR)
SBAS
ERS-1/2
Envisat
COSMO-SkyMed
Landslide
Numerical modelling
Ivancich
Italy

ABSTRACT

We extensively exploit advanced Differential SAR Interferometry (DInSAR) techniques for enhanced landslide investigations. We focus on the Ivancich area, Assisi, Central Italy, which is affected by a deep-seated landslide investigated through in-situ surveys. For this area, large data sets of SAR acquisitions were collected by the C-band ERS-1/2 and ENVISAT sensors (from April 1992 to November 2010), and by the X-band radars of the COSMO-SkyMed (CSK) constellation (from December 2009 to February 2012). We concentrate on the advanced DInSAR technique referred to as Small BAseline Subset (SBAS) approach, benefiting of its capability to generate deformation time series at full spatial resolution and from multi-sensor SAR data. This allows us to present one of the first examples for a landslide area of ERS-1/2 — ENVISAT deformation time series exceeding 18 years. The results allowed characterizing the long-term behaviour of the landslide, and identifying sectors of the unstable slope affected by different deformation dynamics. Analysis of the CSK data set, characterized by a reduced revisit time and improved spatial resolution, resulted in a 15-time larger point density with respect to the ERS-ENVISAT measurements, allowing to investigate nearly all the buildings (and, in many cases, portions of buildings) in the landslide area. Lastly, we present an innovative modelling approach based on the effective integration of the DInSAR measurements with traditional geological and geotechnical information, providing deeper insights on the kinematical evolution of the landslide. We consider our analysis a prototype example that can be extended to different geological and geotechnical conditions, providing significant advances in the understanding of ground deformations induced by active landslides.



## 1. Introduction

Landslides are abundant and frequent phenomena in many regions of the World, where they threaten private and public properties and human life, with significant socio-economic losses (Brabb & Harrod, 1989; Petley, 2012). Understanding the spatial and temporal evolutions of landslides is of primary importance for hazard assessment (Guzzetti, Reichenbach, Cardinali, Galli, & Ardizzone, 2005; Van Westen, Van Asch, & Soeters, 2006) and risk management (Glade, Anderson, & Crozier, 2005; Reichenbach, Galli, Cardinali, Guzzetti, & Ardizzone, 2005), and for the definition, design, and implementation of effective prevention and mitigation strategies. The availability of time series relevant to slope failures (Rossi, Witt, Guzzetti, Malamud, & Peruccacci, 2010; Witt, Malamud, Rossi, Guzzetti, & Peruccacci, 2010) and of ground displacement measurements covering long periods (Angeli, Pasuto, & Silvano, 2000; Corominas, Moya, Ledesma, Lloret, & Gili, 2005; Fastellini, Radicioni, & Stoppini, 2011; Malet, Maquaire, & Calais, 2002; Peyret et al., 2008; Tommasi, Pellegrini, Boldini, & Ribacchi, 2006) allows investigating the history of slope deformations, and deciding on effective remedial works and mitigation efforts (Corsini, Pasuto, Soldati, & Zannoni, 2005; Revellino, Grelle, Donnerumma, & Guadagno, 2010). Ground-based monitoring systems, including distance metres, total stations, Global Positioning System (GPS) receivers, extensometers, tilt-metres, and inclinometers permit monitoring unstable slopes, providing accurate spatial and temporal information on the surface and subsurface displacements of a mass movement (Angeli et al., 2000; Giordan et al., 2013; Petley, Mantovani, Bulmer, & Zannoni, 2005). However, the use of conventional monitoring techniques proves to be difficult and resource intensive, especially where the investigation has to cover large slope failures for long periods (Giordan et al., 2013). The sustainability of a ground-based monitoring network is



* Corresponding author.
*E-mail address:* manunta.m@irea.cnr.it (M. Manunta).

0034-4257/$ – see front matter © 2013 The Authors. Published by Elsevier Inc. All rights reserved.
http://dx.doi.org/10.1016/j.rse.2013.11.003

often hampered by budget and technical limitations, such as inaccessibility of landslide sites, extent of the investigated area and high management costs of the installed instrumentation, limiting the availability of long-term studies of unstable slopes.

Data collected by space-borne Synthetic Aperture Radar (SAR) sensors and processed through Differential SAR Interferometry (DInSAR) techniques represent an important technological advancement for landslide investigations (Bovenga, Wasowski, Nitti, Nutricato, & Chiaradia, 2012; Cascini, Fornaro, & Peduto, 2009, 2010; Guzzetti et al., 2009; Hilley, Bürgmann, Ferretti, Novali, & Rocca, 2004). DInSAR is a remote sensing technique that exploits the phase difference (interferogram) between pairs of SAR acquisitions obtained for the same area at different times and from sufficiently near orbits, allowing to compute displacement maps with centimetre to millimetre accuracy. Developed originally to detect and map the displacements caused by a single natural trigger event, for instance an earthquake (Massonnet et al., 1993) or a volcanic unrest (Massonnet, Briole, & Arnaud, 1995), DInSAR techniques were subsequently extended to generate deformation time series obtained by inverting temporal sequences of DInSAR interferograms (Berardino, Fornaro, Lanari, & Sansosti, 2002; Ferretti, Prati, & Rocca, 2000, 2001; Hooper, 2008; Mora, Mallorqui, & Broquetas, 2003; Werner, Wegmuller, Strozzi, & Wiesmann, 2003). These interferometric approaches, referred to as advanced DInSAR techniques, allow studying the temporal evolution of ground displacements caused by different natural hazards and human activities (Bell, Amelung, Ferretti, Bianchi, & Novali, 2008; Borgia et al., 2005; Dixon et al., 2006; Hilley et al., 2004; Lanari et al., 2010). Advanced DInSAR techniques have improved the measurement precision to about 1–2 mm/year and to 5–10 mm for deformation velocity maps and time series, respectively (Casu, Manzo, & Lanari, 2006; Lanari et al., 2007). This advancement, coupled with the improved temporal sampling of the new SAR sensors, has made advanced DInSAR techniques particularly suitable for landslide investigations, at different scales (Bovenga et al., 2013; Calò, Calcaterra, Iodice, Parise, & Ramondini, 2012; Garcia-Davalillo, Herrera, Notti, Strozzi, & Alvarez-Fernandez, 2013; Hilley et al., 2004; Holbling et al., 2012; Peyret et al., 2008).

With the advent of the "second generation" of X-band SAR systems (e.g., the Italian COSMO-SkyMed (CSK) and the German TerraSAR-X), the mapping and monitoring capabilities of the DInSAR techniques have improved significantly. The SAR images acquired by the new sensors are characterised by reduced repeat cycles (<8 days for COSMO-SkyMed, with the possibility of acquiring data with a 4-day and even 1-day separation) and improved ground resolutions (≤1 m for the COSMO-SkyMed "spotlight" mode, Covello et al., 2010). Improvements in the temporal sampling of the SAR data allow investigating deformation phenomena characterised by highly variable temporal trends. The better spatial resolution results in a significant increase of the number of the measurement points, improving the DInSAR capability of mapping and monitoring landslides (Bovenga et al., 2013, 2012; Iglesias et al., 2012). The improved technological capabilities of the new SAR sensors are of particular interest for site-specific investigations of single landslides (Bovenga et al., 2013; Garcia-Davalillo et al., 2013), and promise to turn the modern DInSAR techniques and their derivative products (i.e., deformation maps, velocity maps, time series of deformations) into valuable additions to the existing traditional (consolidated) monitoring techniques (Giordan et al., 2013). However, an effective integration of DInSAR and traditional monitoring data that fully exploits the characteristics and strengths of the different techniques remains a challenge.

In this work, we show the relevance of the advanced DInSAR techniques for the investigation of active landslides. For the purpose, we exploit the advanced SBAS-DInSAR approach (Berardino et al., 2002; Lanari et al., 2004) and we apply it to the Ivancich landslide that affects part of the Assisi urban area, Central Italy. The Ivancich landslide is an ideal test site because of the large availability of in-situ surface and sub-surface information, and of large data sets of C-band and X-band SAR data. In particular, we demonstrate the importance of the very large stacks of C-band SAR data acquired by the ERS-1/2 and the ENVISAT satellites for the production of long deformation time series covering almost two decades, to characterise the long-term behaviour of the landslide. Next, we show the improved capability of the new generation of X-band SAR sensors (e.g., the COSMO-SkyMed sensors) for accurate spatial and temporal analyses of the surface deformations caused by the active landslide in an urbanised area. Lastly, we show how DInSAR measurements can be used in combination with geological and geotechnical information to explore the slope stress-strain state and the landslide kinematic evolution by means of a Finite Element Method (FEM) modelling approach. The proposed model was optimised through a calibration of the numerical results with the available monitoring data, by adopting an inverse analysis method (Manconi et al., 2010; Tizzani et al., 2010), and provided new insights on the kinematical evolution of the slope failure. We conclude discussing the achieved results and their potential application in other landslide areas.

## 2. Rationale for the SBAS-DInSAR approach

Among the advanced DInSAR techniques developed in the last decade (Berardino et al., 2002; Ferretti et al., 2000, 2001; Hooper, 2008; Mora et al., 2003, Werner et al., 2003), the Small BAseline Subset (SBAS) technique (Berardino et al., 2002) exploits SAR image pairs characterised by short temporal and spatial orbital separations (baseline) to limit "decorrelation" (noise) effects, and to maximise the number of coherent SAR targets (point scatterers) detected on the ground. Originally designed to investigate deformation phenomena affecting large to very large areas, the technique was extended to analyse local phenomena (Manunta et al., 2008), including slope failures (Bovenga et al., 2013, 2012; Calò et al., 2012; Guzzetti et al., 2009). The technique is particularly well suited to detect and measure displacements with a non-linear variation in time, a feature of specific interest for landslide studies, since landslides are known to behave non-linearly, in space and time (Hergarten & Neugebauer, 1998; Rossi et al., 2010).

A peculiarity of the SBAS approach is the fact that the technique can be applied at two spatial scales: the regional and the local scales (Lanari et al., 2004). At both scales, the technique generates the same products (i.e., deformation maps, velocity maps, time series of deformations), albeit with different spatial resolutions. At the regional scale, the technique exploits average (i.e., multi-look) interferograms to obtain deformation velocity maps, and associated time series, covering large to very large areas (from a few hundreds to several thousands of square kilometres) with a coarse ground resolution (e.g., approximately 100 m × 100 m when using ERS-1/2 and ENVISAT data, and approximately 30 m × 30 m when using COSMO-SkyMed data). At the local scale, the technique uses single-look interferograms obtained at full resolution (typically 4 m × 20 m for the ERS-1/2 and ENVISAT data, and 3 m × 3 m for the Stripmap COSMO-SkyMed data) to detect local deformations affecting single structures (e.g., a building or a portion of a building, Manunta et al., 2008), single slopes or specific portions of a slope.

The original SBAS technique (Berardino et al., 2002) was extended to exploit SAR data captured by different radar systems that acquire with the same illumination geometry, e.g., the ERS-1/2 and ENVISAT systems (Bonano, Manunta, Marsella, & Lanari, 2012; Pepe, Sansosti, Berardino, & Lanari, 2005). The multi-sensor approach considers images acquired by the ERS-1/2 and ENVISAT sensors as belonging to independent subsets, and cross-interferograms (ERS/ENVISAT) are not generated. The integration of ERS/ERS and ENVISAT/ENVISAT sequences of interferograms is performed at the stage of the generation of the time series of deformations, merging the two independent time series obtained by processing the ERS and the ENVISAT acquisitions (Pepe et al., 2005). As a result, the SBAS technique can now be used to obtain deformation maps and associated time series spanning very long periods (decades),

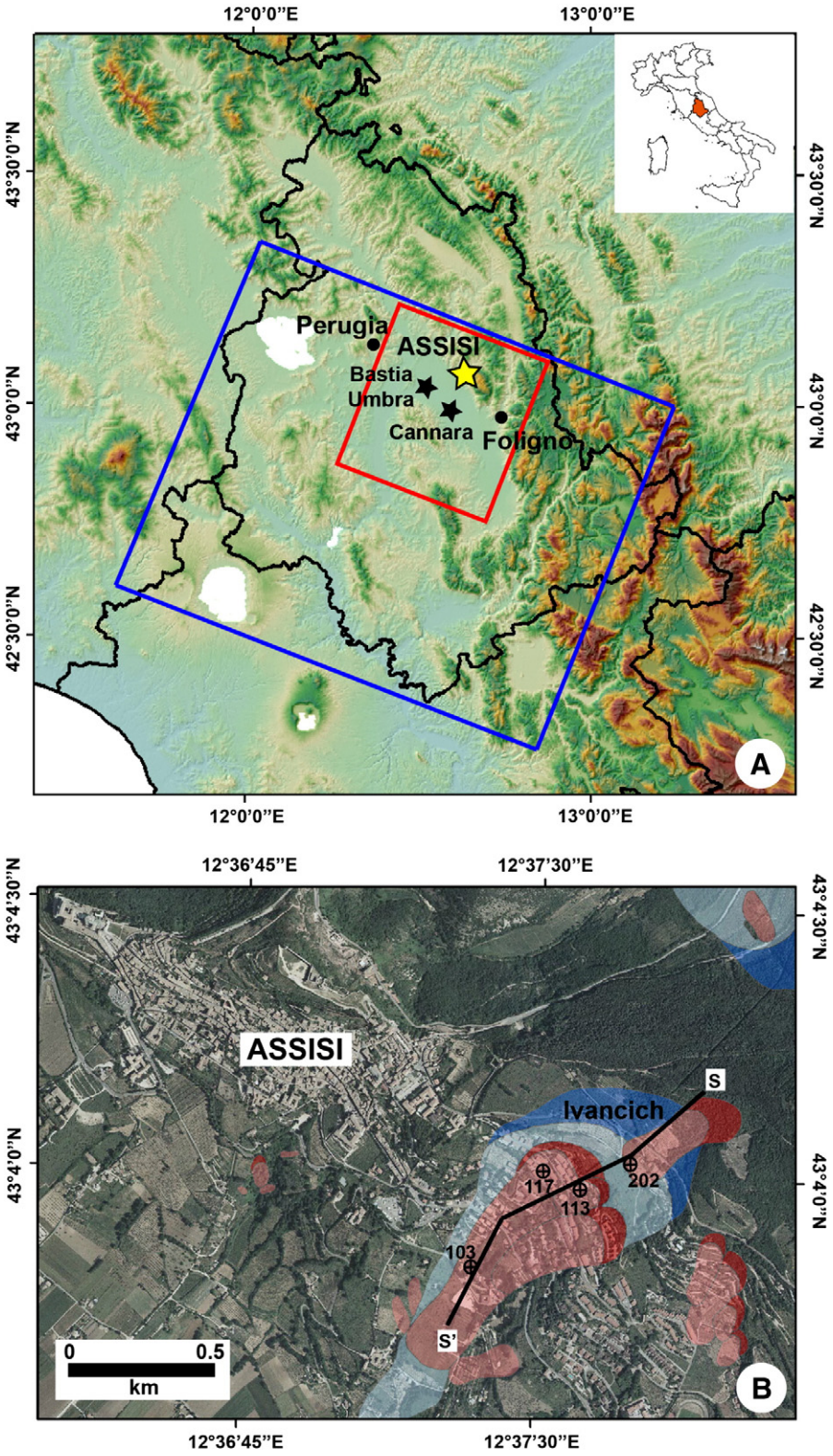


**Fig. 1.** Location of the study area. (A) Map showing terrain morphology in Umbria, Central Italy. Yellow star shows localization of the Ivancich study area (Assisi). Black stars show localization of the Bastia Umbra and Cannara rain gauges. Coloured polygons show footprints of the descending ERS-1/2 and ENVISAT (blue), and COSMO-SkyMed (red) data used in the study. (B) Landslide inventory map for part of the Assisi municipality (modified from Antonini et al., 2002). Shades of blue show ancient and relict landslides, and shades of red show recent landslides. The landslide crown areas (darker colours) are mapped separately from the landslide deposits (lighter colours). Black crossed circles show location of inclinometers. Thick black line shows the longitudinal cross section S–S' used for modelling (see Figs. 9, 10, 11).

providing unprecedented information for studying long-term ground displacements. The capacity is of particular interest for landslide investigations, as it allows preparing very long time series of displacements for single or multiple points on the topographic surface. This premium information is seldom available to landslide investigators (Giordan et al., 2013).

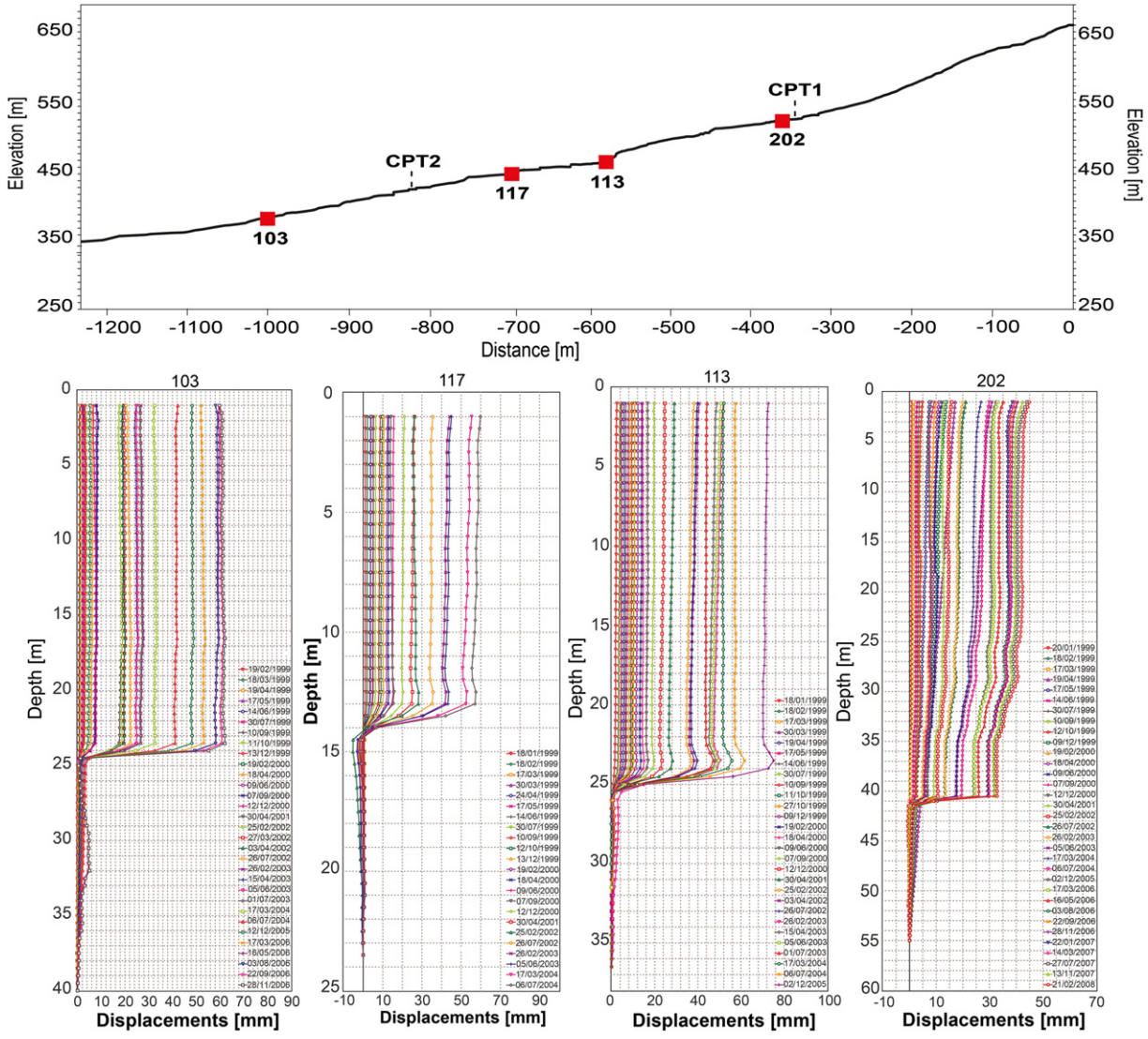


**Fig. 2.** Top: topographic profile along the unstable slope, and location of inclinometers. CPT1 and CPT2 indicate direction changes of the profile trace. Bottom: inclinometer measurements for the 103, 113, 117 and 202 inclinometers.

The full resolution multi-sensor SBAS approach also exploits the Doppler centroid variations of the post-2000 ERS-2 acquisitions, and the carrier frequency difference between the ERS-1/2 and the ENVISAT systems. This information is used to identify the coherent SAR pixels exhibiting a response that deviates significantly from a single-scatterer backscattering, and to improve the geocoding of the scatter points (Bonano et al., 2012). Moreover, because some of the SAR images acquired by the COSMO-SkyMed sensors are characterised by a significant Doppler centroid offset (Bonano, Manunta, Pepe, Paglia, & Lanari, 2013), the full-resolution SBAS approach exploits this information to improve also the final geocoding of the coherent COSMO-SkyMed pixels (Bonano et al., 2012). The improved ability to accurately geocode the SAR coherent targets is important for landslide studies, where the surface deformation can vary irregularly from point to point in response to local conditions (e.g., the presence of a geological or geomorphological boundary, the presence of human made structures that respond differently to the landslide movement).

## 3. Study area

For our experiment, we selected the Ivancich test site, in the Assisi municipality, Umbria, Central Italy (Fig. 1A). The Ivancich residential neighbourhood extends to the E of the mediaeval part of the town, and is affected by a known active landslide (Fig. 1B). The landslide has been the subject of geological and engineering investigations since the late 1970s, when roads, and private and public buildings, including a new hospital, were damaged (Angeli & Pontoni, 2000; Canuti, Marcucci, Trastulli, Ventura, & Vincenti, 1986; Felicioni, Martini, & Ribaldi, 1996; Pontoni, 2011). The Assisi local government and the Umbria regional government have made several efforts to define and characterise the unstable area, to monitor the active landslide, and to design and implement effective remedial works. As part of this long-term effort, the Ivancich landslide was monitored from 1982 to 2008 with topographic and inclinometer measurements (Fastellini et al., 2011; Pontoni, 1999, 2011). Geomorphological and geotechnical investigations and repeated topographical surveys revealed that the mass movement is an old translational slide with a rotational component in the source area. The movement develops along the slope (Fig. 2) from an elevation of 660 m a.s.l. to an elevation of 350 m a.s.l. and involves a debris deposit, 15 to 60 m in thickness, that overlays the bedrock represented by a pelitic–sandstone unit and layered limestone (Angeli & Pontoni, 2000; Canuti et al., 1986; Cardinali, Antonini, Reichenbach, & Guzzetti, 2001; Servizio Geologico Italiano, 1980). Inclinometer measurements (Fig. 2) performed between 1998 and 2008 revealed that the shear zone separating the landslide material from the stable bedrock is relatively thin (<2 m), and that the bulk of the material above the shear

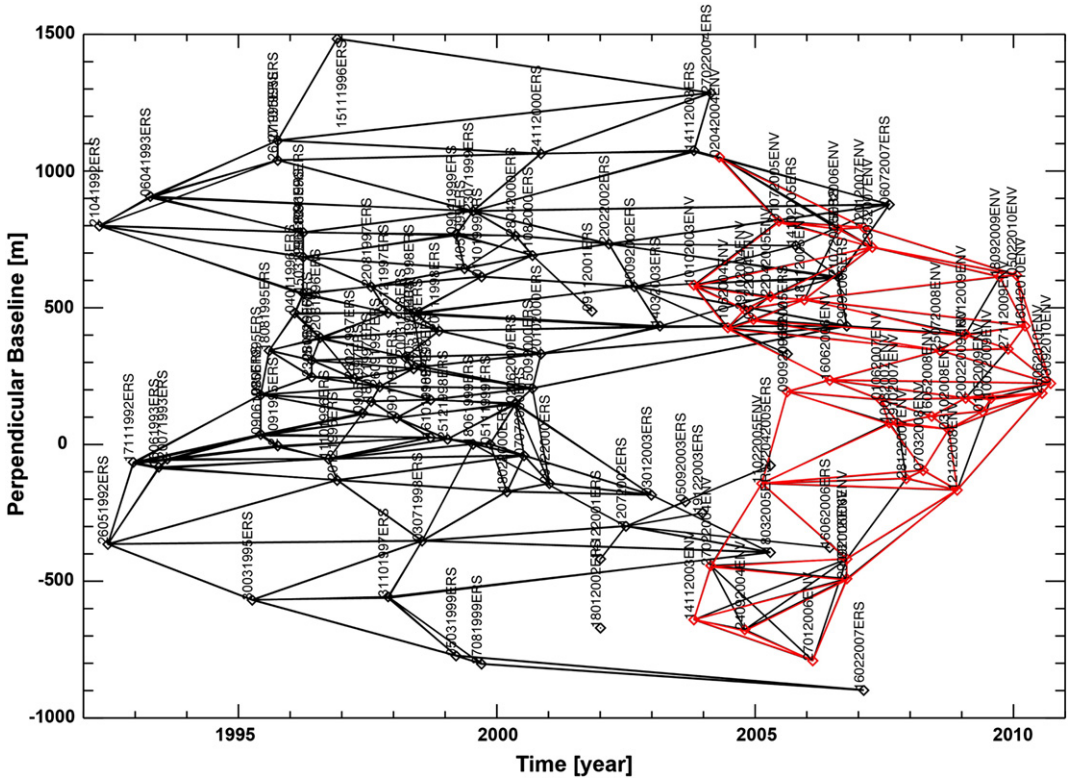


**Fig. 3.** Distribution of ERS-1/2 (black) and ENVISAT (red) acquisitions used for the analysis, in the temporal (x-axis)–perpendicular (y-axis) baseline plane. Black diamonds are single ERS-1/2 images. Red diamonds are single ENVISAT images. Black lines show individual ERS/ERS interferograms. Red lines show individual ENVISAT/ENVISAT interferograms.

zone moves as a nearly rigid body (Angeli & Pontoni, 2000; Pontoni, 2011).

## 4. SBAS-DInSAR analysis

### 4.1. Available SAR data

To investigate the ground deformations in the Ivancich landslide area (Fig. 1B), we used two sets of SAR images. The first set consisted of 91 ERS-1/2 and 39 ENVISAT, C-band images taken between 21 April 1992 and 12 November 2010 (18.6 years) along the satellites descending orbits, with a 35-day revisit time and a spatial resolution of about 10 m. The second set consisted of 39 COSMO-SkyMed, X-band images taken between 2 December 2009 and 22 February 2012 (26 months), also along descending orbits with a 7-day revisit time and a 3 m × 3 m spatial resolution.

### 4.2. Long-term C-band measurements

We used the 91 ERS-1/2 and the 39 ENVISAT acquisitions to generate 347 interferograms, including 230 ERS/ERS and 117 ENVISAT/ENVISAT interferograms. To produce the interferograms, we selected pairs of SAR acquisitions that satisfied the following conditions: (i) a spatial baseline (i.e., the perpendicular distance between the two orbits) <400 m, and (ii) a temporal baseline (i.e., the separation in time between two images) <1500 days (Fig. 3). For the processing, we used precise information on the satellite orbits obtained from the German Aerospace Center (Deutsches Zentrum für Luft-und Raumfahrt, DLR), and topographic information obtained from the Digital Elevation Model (DEM) with a 3-arc-second spacing (approximately 90 m × 90 m) produced by the Shuttle Radar Topography Mission (SRTM) in February of 2000. The coarse resolution DEM was used to estimate and subtract the topographic phase component from the computed interferograms, to single out information relevant to the ground deformations in the study area.

The multi-scale SBAS approach allows performing analyses at regional and local scales, exploiting multi-look (averaged) and single-look (full-resolution) interferograms. For a complex multi-look processing, we used 4 looks in the range direction and 20 looks in the azimuth direction. Considering that the pixel size of the ERS-1/2 and ENVISAT images is about 20 m (ground range) × 4 m (azimuth), the averaged result consisted in interferograms with a ground resolution of about 80 m × 80 m. Conversely, the local scale SBAS analysis was performed using the full-resolution single-look interferograms.

Application of the SBAS-DInSAR approach to the C-band (ERS and ENVISAT) images resulted in the production of ground deformation maps and associated time series covering the 18.6-year period from April 1992 to November 2010 (Fig. 4). This period is longer than the 8.7-year period (April 1992–December 2000) used by Guzzetti et al. (2009) to investigate landslides in the same general area, and longer than the 6.6-year period (October 2003–May 2010) used by Bovenga et al. (2013) to investigate the Ivancich landslide. The significantly longer observation period allows a better understanding of the long-term dynamic behaviour of the Ivancich landslide.

Inspection of the full resolution deformation map (Fig. 4A) and the associated time series (Fig. 4B) reveals that the Ivancich landslide, classified as active in the regional landslide inventory map of Antonini et al. (2002) (Fig. 1B), comprises sectors characterised by different displacement rates and patterns. Particularly interesting is the active sector in the NW part of the landslide that has suffered cumulated displacements exceeding locally 15 cm, corresponding to an average displacement rate of 8 mm/year. The result is in general agreement with the outcomes of a reconnaissance survey carried out on 6 September 2011 to detect the damage caused by the moving landslide. The survey revealed that damage was most severe along the boundary between the active landslide sector and the portion of the slope not affected by

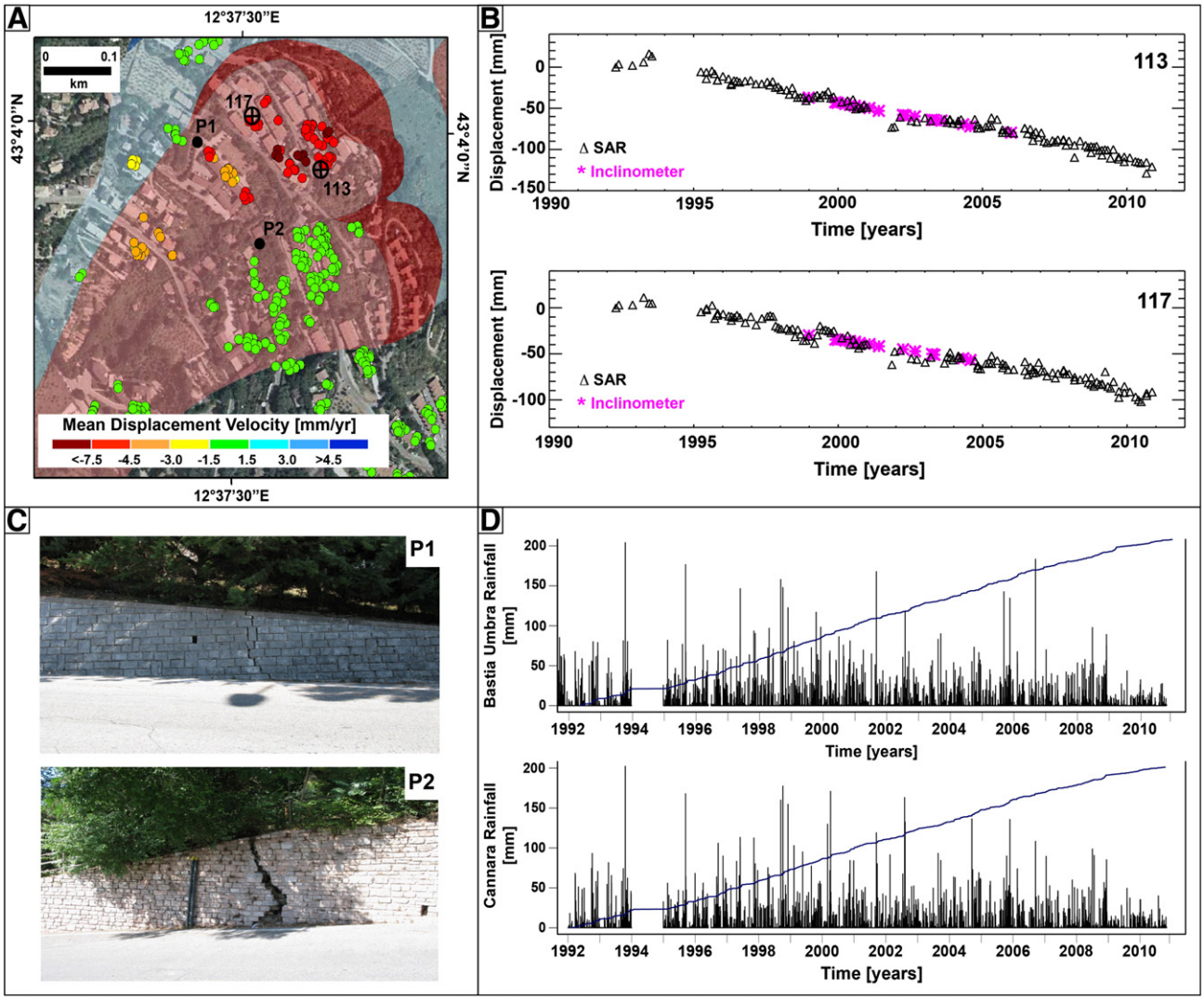


**Fig. 4.** SBAS-DInSAR processing results of C-band (ERS-1/2 and ENVISAT) SAR data between April 1992 and November 2010 for the Ivancich landslide, Assisi. (A) Full resolution (pixel size ≈ 20 m along azimuth × 4 m along range) deformation velocity map, superimposed on the landslide inventory map (see Fig. 1B for legend). Displacements measured along the satellite Line of Sight (LOS). (B) Time series of deformation for two unstable scatter points (black triangles) and two inclinometers (purple stars) in the active landslide sector. For location of the two inclinometers see 113 and 117 in (A). The inclinometer measurements are projected along the satellite LOS. (C) Examples of damage in the Ivancich landslide area. Photographs taken on 6 Sep 2011. For location of the damage see P1 and P2 in (A). (D) Rainfall measurements and monthly cumulative rainfall for the Bastia Umbria and Cannara rain gauges. See Fig. 1A for location of the rain gauges.

displacements (Figs. 4A, C). Inspection of the history of deformation for two scatter points located in the active landslide (Fig. 4B) confirms the quasi-linear displacement rate of the Ivancich active slide (Guzzetti et al., 2009), in the observation period.

Information on the sub-surface geometry of the Ivancich landslide is available from boreholes and inclinometer measurements (Angeli & Pontoni, 2000; Pontoni, 2011). We used this in-situ information to investigate the accuracy of the DInSAR measurements. For the purpose, we compared the DInSAR measurements to those recorded by two inclinometers installed in the NE (113) and the NW (117) parts of the upper portion of the landslide area (Figs. 1B, 2, 4B). For the 113 inclinometer, the measurements covered the 7-year period from December 1998 to December 2005 with a cumulated displacement at the ground surface of 75 mm (approximately 11 mm/year). For the 117 inclinometer, the measurements cover the 5.6-year period from December 1998 to July 2004 with a cumulated displacement at the ground surface of 59 mm (approximately 10 mm/year). To compare the two types of data (inclinometer and DInSAR), the inclinometer measurements were projected along the Radar Line Of Sight (LOS), considering the orbital information of the SAR data and the local topography (i.e., the slope information retrieved from the SRTM DEM). The result of the comparison is shown in Fig. 4B where the inclinometer measurements projected along the satellite LOS (purple stars) are superimposed on the corresponding SBAS-DInSAR deformation time series (black triangles). The agreement between the DInSAR and the inclinometer data is clear. We further computed the standard deviation $\sigma$ of the differences between the two time series of independent measurements, obtaining $\sigma = 5$ mm for the 113 inclinometer and $\sigma = 4$ mm for the 117 inclinometer. These results are consistent with other independent analyses on the quality of the SBAS-DInSAR technique and the derivative products (Bonano et al., 2012, 2013; Casu et al., 2006; Lanari et al., 2007).

Rainfall is a driver for the Ivancich landslide (Angeli & Pontoni, 2000; Pontoni, 2011). Ardizzone et al. (2011) performed an analysis of the temporal relationship between the local rainfall record and the history of ground deformations in the Ivancich landslide area (Figs. 4B, D). In particular, Ardizzone et al. (2011) considered the surface displacement measurements obtained through DInSAR processing of C-band ERS-1/2 and ENVISAT images in the 18.4-year period from April 1992 to September 2010, and rainfall measurements acquired by two rain gauges located 5.5 km W and 9 km SSW from the Ivancich landslide, for the same period (Figs. 1A, 4D). The performed cross-correlation analysis, based on monthly-cumulated rainfall, revealed a lack of temporal correlation

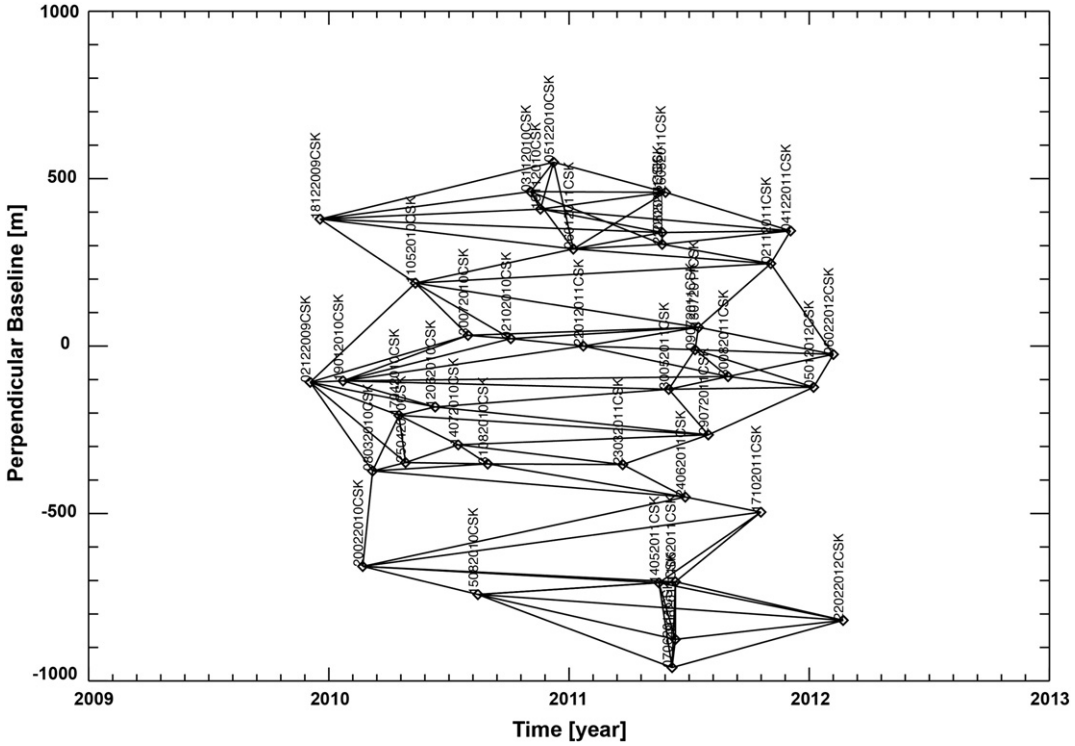


**Fig. 5.** Distribution of COSMO-SkyMed acquisitions used for the analysis in the temporal (x-axis)–perpendicular (y-axis) baseline plane. Black diamonds are single images, and black lines show individual interferograms.

between landslide deformations and rainfall. We extended the analysis considering the rainfall cumulated over different time periods (7, 15, and 90 days), and obtained cross-correlation values <0.2, confirming the lack of a clear relationship between landslide displacements and local rainfall history (Ardizzone et al., 2011).

Unpublished piezometer data acquired in the landslide deposit reveal that the groundwater regime affects quite moderately the landslide kinematics. In particular, the ground water surface was measured to be, in general, only a few metres above the shear band. This results in very low piezometric heights, when compared to the total stress levels. Also, the piezometric surface was observed to be approximately constant in time, with limited seasonal fluctuations. We consider this a further indication of the limited influence of the rainfall pattern and of the slope groundwater regime on the landslide kinematics, which is characterised by displacement rates approximately constant in time over long periods.

### 4.3. Spatially dense X-band measurements

We used the 39 CSK acquisitions to generate 110 interferograms collectively covering the 26-month period between December 2009 and February 2012. For this analysis, we selected pairs of images that satisfied the criterion of having a spatial baseline of <300 m (Fig. 5). No constrain was imposed to the temporal separation between the acquisitions. For the complex multi-look processing, we used 10 looks in the range and in the azimuth directions, obtaining averaged interferograms with a pixel size of about 30 m × 30 m.

We focus on the results of the full resolution processing for the urban area of Assisi (Fig. 6), and specifically for the Ivancich neighbourhood. Visual comparison of the results obtained processing the X-band, CSK data (Fig. 6A) with the results achieved processing the C-band, ERS-1/2 and ENVISAT data (Fig. 6B) reveals that the two analyses resulted in very similar spatial patterns of deformations, for two different periods: (i) 18.6 years between April 1992 and November 2010 for the ERS-1/2 and ENVISAT data, and (ii) 26 months between December 2009 and February 2012 for the CSK data. We maintain that this is consistent with the quasi-linear trend of displacement of the Ivancich landslide.

Comparison of Figs. 6A and B reveals a significantly larger density of coherent points detected by the CSK data, compared to the ERS-1/2 and ENVISAT data. This is in agreement with similar findings by Bovenga et al. (2012, 2013) in landslide areas, and by Bonano et al. (2013) in urban areas. Processing of the shorter X-band, CSK data series resulted in the identification of 30,000 coherent points in the area covered by Fig. 6A, corresponding to an average density of about 15,000 points/km$^2$. This compares to 2000 coherent points detected in the same area by processing the significantly longer C-band, ERS-1/2 and ENVISAT data series, for an average density of 1000 points/km$^2$ (Fig. 6B). The 15-time increase in the spatial density of coherent points is particularly significant to investigate the Ivancich landslide, allowing for a more detailed analysis of the spatial distribution of the ground deformations.

Close inspection of Fig. 6A reveals trends in the pattern of the deformation (shown by the spatial variation in the red and orange colours) that are not visible in Fig. 6B. This is emphasised in Fig. 7 where the displacements measured along three profiles are compared. The A–B profile, 362 m in length across the active landslide, shows a clear variation in the displacement rate across the landslide deposit, and outlines a distinct band of deformation of about 50 m in width along the NW boundary of the landslide. The sparse ERS-1/2 and ENVISAT scatter points (purple triangles) did not detect the variation in the surface velocity across the landslide deposit. The C–D profile, 500 m in length along the active landslide, also shows distinct variations in the surface displacement rate, with faster movements (red colours) in the upper part of the landslide and slower movements (orange colours) in the lower part of the investigated area.

The considerably larger density of coherent points detected processing the CSK data is particularly significant in urban areas, where buildings and other structures and infrastructures are abundant. In Fig. 7, the E–F profile, 80 m in length, crosses longitudinally a set of two-storey, masonry buildings typical of the Ivancich neighbourhood. Close inspection of the E–F profile reveals variations in the rate of displacement between buildings, and even within individual buildings. This characteristic, distinctive of the high-resolution X-band data, is particularly relevant for the definition of the spatial pattern of the deformations. Moreover, such

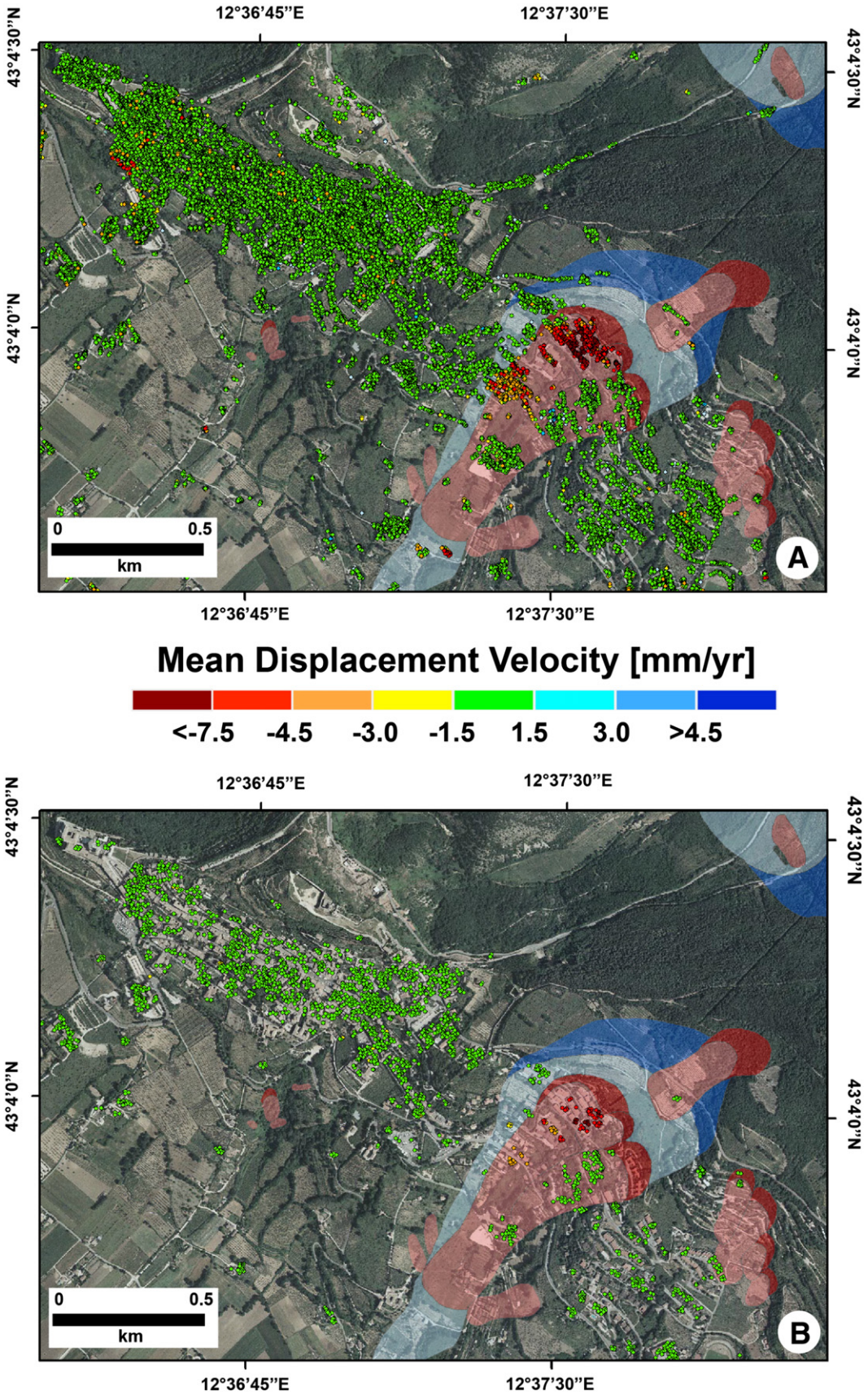


**Fig. 6.** Full resolution, ground deformation velocity maps obtained through SBAS-DInSAR processing of SAR images for Assisi superimposed on the landslide inventory map (see Fig. 1B for legend). Displacements measured along the satellites Line of Sight (LOS). (A) Deformation velocity map obtained processing 39 X-band SAR images taken by the COSMO-SkyMed satellites in the 26-month period from December 2009 to February 2012. (B) Deformation velocity map obtained processing 130 C-band SAR images taken by ERS-1/2 and ENVISAT satellites in the 18.6-year period from April 1992 to November 2010.

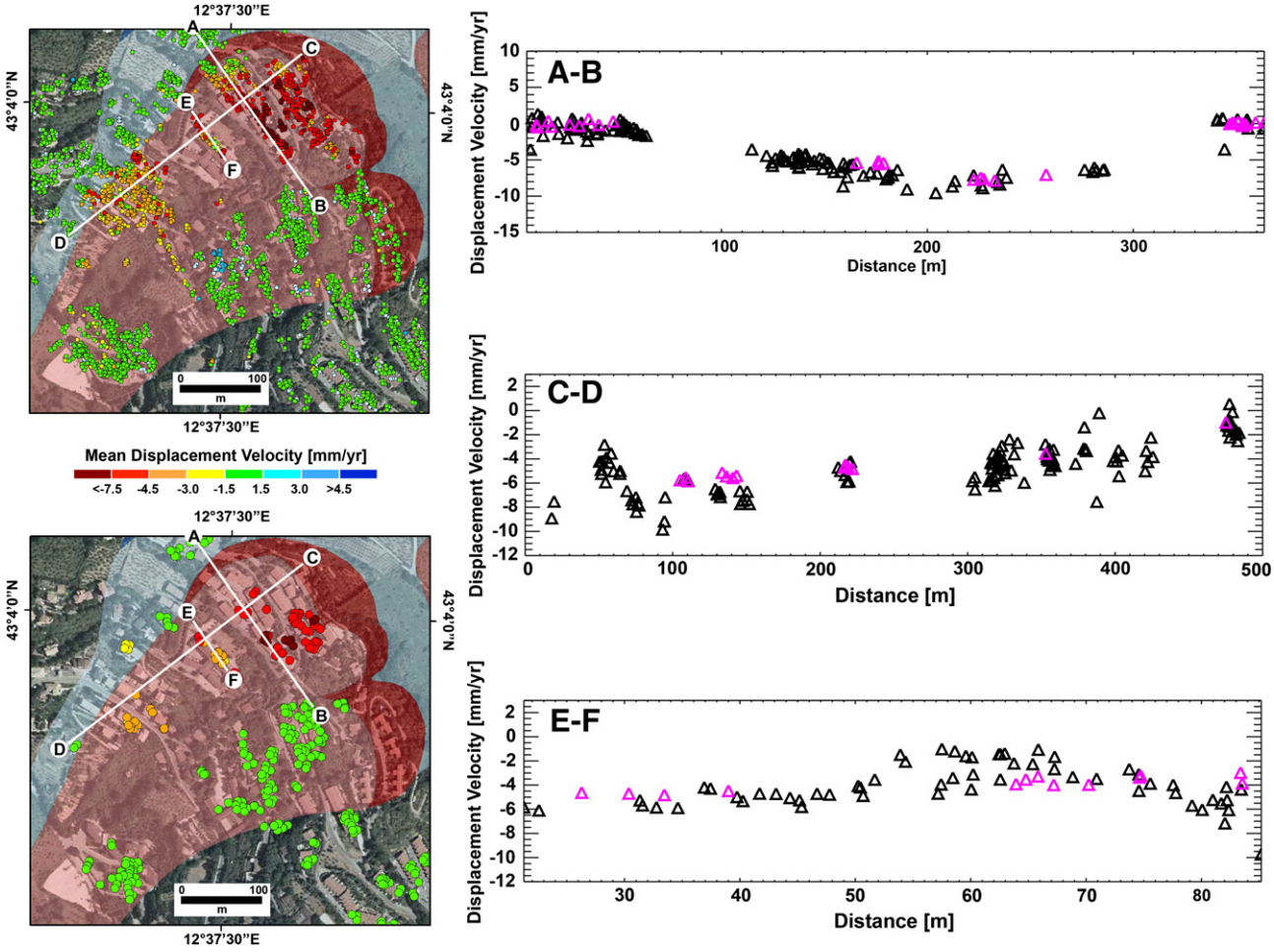


**Fig. 7.** Full resolution, ground deformation velocity maps obtained through SBAS-DInSAR processing of SAR images for the Ivancich area, Assisi, superimposed on the landslide inventory map (see Fig. 1B for legend). Displacements measured along the satellites Line of Sight (LOS). White lines show traces of profiles. In the graphs, black and purple triangles represent COSMO-SkyMed and ERS-ENVISAT scatter points, respectively. Upper map shows displacement velocity obtained processing 39 X-band SAR images taken by the COSMO-SkyMed satellites in the 26-month period from December 2009 to February 2012. Lower map shows displacement velocity obtained processing 130 C-band SAR images taken by ERS-1/2 and ENVISAT satellites in the 18.6-year period from April 1992 to November 2010.

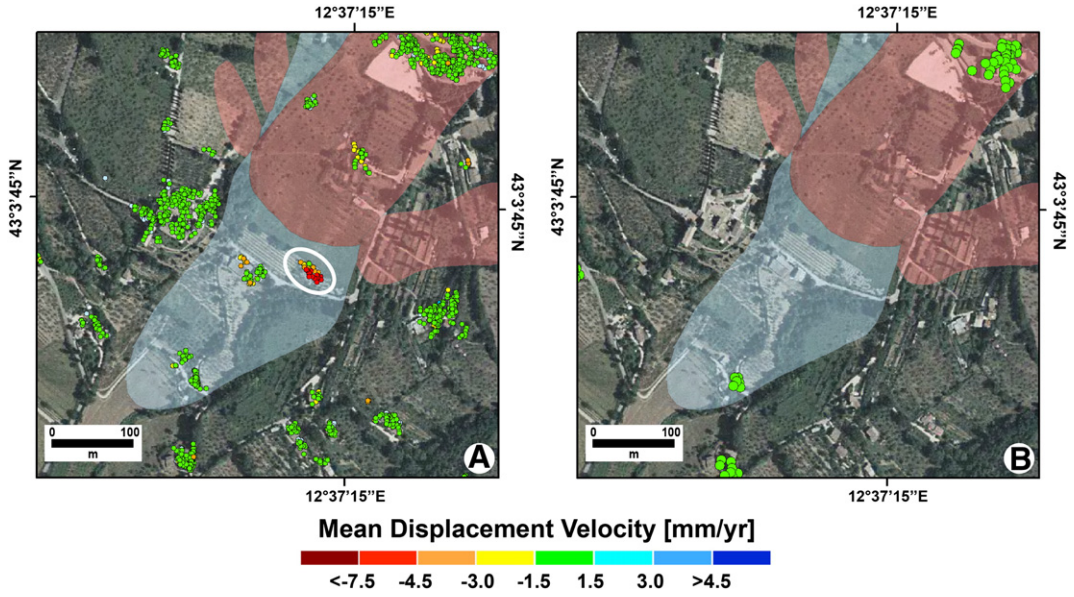


**Fig. 8.** Full resolution, ground deformation velocity maps for the toe of the Ivancich landslide obtained through SBAS-DInSAR processing of COSMO-SkyMed (A) and ERS-1/2 and ENVISAT (B) SAR images. Displacements measured along the satellites Line of Sight (LOS).

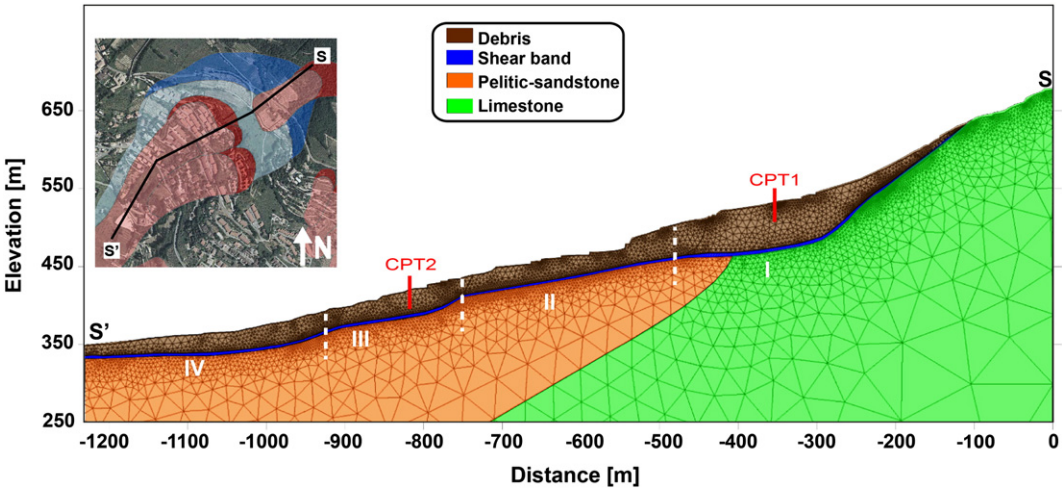


**Fig. 9.** Two-dimensional model geometry with geological units superimposed on the triangular modelling mesh. Inset shows the modelled longitudinal cross section S–S'. I, II, III and IV represent four shear band sectors. CPT1 and CPT2 indicate direction changes of the profile trace.

characteristic is also important to support the design of effective remedial measurements, and to monitor their efficiency.

As a final remark, we emphasize the possibility offered to by the CSK DInSAR-SBAS analysis to detect the effects of ground deformations not revealed by the previous ERS-ENVISAT processing. This is demonstrated in Fig. 8 that shows a building located on the toe of the Ivancich landslide. Such building is clearly affected by displacements that were detected and measured by processing the X-band CSK data (Fig. 8A), and were not detected by processing the C-band ERS-ENVISAT data (Fig. 8B).

## 5. Landslide modelling using DInSAR measurements and sub-surface data

In this section, we discuss the use of the spatially dense CSK DInSAR measurements, in conjunction with independent geological, geomorphological, and geotechnical information, for the two-dimensional modelling of the kinematical evolution of the Ivancich active landslide (Fig. 1B). In this paper, our modelling approach is based on the simulation of the materials undergoing shear strain as Newtonian fluids. For the modelling, the geometry of the topographic surface was defined based on the available topographic maps, and the sub-surface geological setting was determined according to the available borehole information and the local geology. The geometry of the shear band delimiting the landslide mass was determined from in-situ geomorphological evidences, and from the depth and thickness of the shear deformation measured in the inclinometers installed in the landslide deposit (Fig. 2). The material properties were obtained from existing geotechnical investigations (Angeli & Pontoni, 2000; Pontoni, 1999). Next, by assuming Newtonian viscosities for the materials involved in the failure, a kinematical analysis was performed. The viscosity parameters were obtained through the same FEM simulations by adopting an "inverse analysis" approach. Specifically, the approach optimised the viscosity parameters in order to obtain the best-fit between the simulated slope kinematics and the SAR measurements of the surface displacement rates, as described below.

We performed the two-dimensional modelling along the longitudinal cross section S–S' traced in the centre of the landslide (Fig. 1B), and we subdivided the modelling domain into four geo-mechanical units, namely (Fig. 9): (i) the landslide deposit, consisting chiefly of unsorted debris, (ii) the limestone bedrock, in the upper part of the slope, (iii) the pelitic–sandstone bedrock, in the central and the lower parts of the slope, and (iv) the shear zone, characterised by a thickness lower than 2 m and a depth between 15 and 60 m. The stress state in the slope and the distribution of the shear stresses in the slope were first defined by an elastic analysis under gravitational loading, for which we adopted the unit weight and the elastic parameters of the materials listed in Table 1. To simplify our analysis and to reduce the computation time, we considered four nearly homogeneous sectors along the landslide shear band (Fig. 9). This hypothesis is supported by the analysis of DInSAR measurements that allowed us to identify four areas characterised by a similar kinematical behaviour. In addition, the partition of the shear band in four different sectors is consistent with the geomorphological evidences of the presence of inner landslide deposits, which are part of the larger Ivancich landslide, with crests at different elevation and inclination of the shear band.

For the comparison of the numerical modelling with the monitoring data, we considered all the CSK coherent pixels located within a distance of 20 m from the representative longitudinal cross section S–S'. The long-term DInSAR analysis revealed a quasi-linear trend of displacement for the active landslide (Section 4.2, Fig. 4B). As already shown in Section 4.2, this kinematical trend was confirmed by the analysis of inclinometric measurements performed in different boreholes (Angeli & Pontoni, 2000), which also revealed that the shear deformation concentrates within a narrow zone, so that the overlying landslide debris is moving approximately as a rigid body (Fig. 2).

We solved the Navier–Stokes equations that relate the viscosity field to the velocity field using the Comsol Multiphysics Finite Element Model code (http://www.comsol.com/). To back-calculate the values of the viscosity of the materials in the shear band, an optimization procedure based on a genetic algorithm (Manconi et al., 2010; Tizzani et al., 2010) was used to derive the best fit, within a quadratic norm, between the displacement velocities computed by the model and the CSK displacement rates. A good fit was obtained by assuming the four sectors of the shear band defined above (Fig. 9) as characterised by different dynamic viscosities ($\mu_1$, $\mu_2$, $\mu_3$, and $\mu_4$) (Fig. 10A). The following values of the Newtonian viscosities were derived [MPa × s]: $\mu_1 = 7.5 \times 10^{10}$, $\mu_2 = 3.0 \times 10^{8}$, $\mu_3 = 1.0 \times 10^{8}$, and $\mu_4 = 1.2 \times 10^{9}$.

**Table 1**
Physical and mechanical properties of the geo-mechanical units used for the Finite Element Modelling of the Ivancich landslide.

| Rock material | Density [kN/m$^3$] | Young's modulus [MPa] | Poisson ratio [−] |
|---|---|---|---|
| Limestone bedrock | 22 | $8 \times 10^3$ | 0.28 |
| Pelitic–sandstone bedrock | 18.5 | $7 \times 10^3$ | 0.26 |
| Debris deposit | 16 | $1 \times 10$ | 0.24 |
| Alluvial deposit | 17 | $6 \times 10$ | 0.24 |
| Shear band | 16 | $1 \times 10$ | 0.23 |

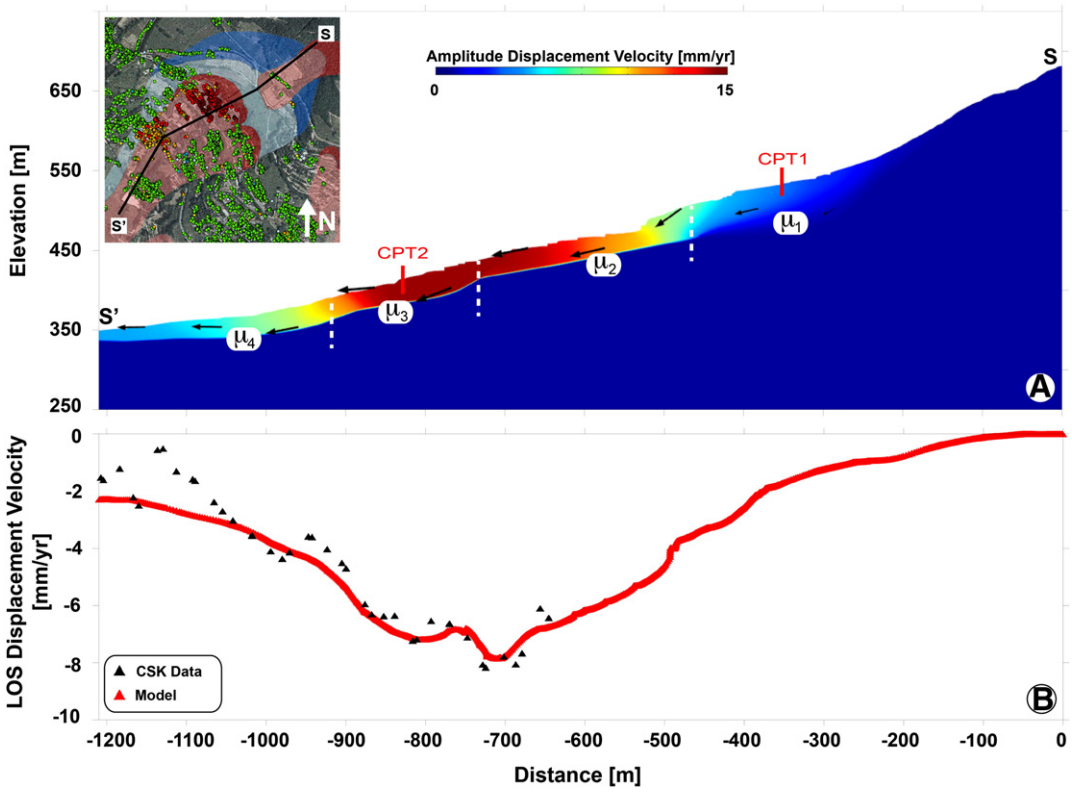


**Fig. 10.** (A) Two-dimensional displacement field obtained from numerical modelling along the longitudinal cross section S–S' of the Ivancich landslide. μ1, μ2, μ3 and μ4 are the dynamic viscosities for the four shear band sectors. CPT1 and CPT2 indicate direction changes of the profile trace. Inset shows the modelled longitudinal cross section S–S', superimposed on the full resolution, ground deformation velocity map obtained processing COSMO-SkyMed data. (B) Comparison between the modelled velocity profile (red triangles) and the COSMO-SkyMed measurements (black triangles) along the longitudinal cross section of the landslide.

The resulting velocity field along the modelled landslide section is shown in Fig. 10. We observe that the viscosity values decrease markedly in the central part of the shear band ($\mu_2 = 3.0 \times 10^8$ MPa × s, $\mu_3 = 1.0 \times 10^8$ MPa × s), where the shear deformation is largest, whereas in the upper and in the lower areas of the shear band the viscosities are larger ($\mu_1 = 7.5 \times 10^{10}$ MPa × s, and $\mu_4 = 1.2 \times 10^9$ MPa × s, respectively). Values of the viscosity significantly higher than those in the shear zone were assigned to the landslide debris to obtain significantly lower shear rates in the region overlying the shear surface. This is in agreement with the available inclinometric data (Fig. 2).

The model allowed studying the magnitude and the direction of movement in the active landslide. This was achieved by investigating the horizontal and the vertical components of the movement. In Fig. 11 we show the modelled horizontal velocity of movement, and we compare this modelled information to the inclinometer data obtained from four boreholes located in different parts of the active landslide (Fig. 11B). The agreement between the modelled and the measured (in the boreholes) horizontal velocities is good, except for the 117 inclinometer. For this inclinometer, we attribute the difference between the measured and the modelled velocity to the location of the borehole, which is positioned at a distance of about 150 m to the W of the cross section used for the numerical modelling. Lateral variations in the geometry of the landslide justify the observed difference.

## 6. Discussion

The experiment we have conducted in the Ivancich landslide area, in the Assisi municipality, has shown that the modern DInSAR techniques are particularly well suited to detect and monitor active landslides in urban and sub-urban areas, and to conduct advanced landslide modelling.

First, we exploited the capability of the advanced SBAS-DInSAR technique to process multi-sensor SAR data to present one of the first examples of joint ERS-1/2 and ENVISAT deformation map and associated time series for an active landslide in an urban area (Fig. 4). Specifically, the experiment has shown that the exploitation of the very large archive of ERS-1/2 and ENVISAT data allowed producing maps (Fig. 4A) and time series (Fig. 4B) covering a period of unparalleled length: almost two decades between 1992 and 2010. This is an important and quite rare information for landslide studies (Angeli et al., 2000; Giordan et al., 2013; Malet et al., 2002; Peyret et al., 2008). We compared the DInSAR time series to measurements obtained by two inclinometers located in the Ivancich landslide, available for different periods between December 1998 and December 2005. For consistency, the inclinometer measurements were projected along the satellites LOS. The results (Fig. 4B) proved the accuracy of the DInSAR measurements compared to the inclinometric measurements, and revealed a quasi-linear temporal behaviour of the landslide deformation in the long observation period (18.6 years), with a velocity locally exceeding 8 mm/year. This is a valuable information for the selection of the most appropriate remedial works (Corsini et al., 2005; Revellino et al., 2010).

The ERS-1/2 and ENVISAT data used to investigate the Ivancich landslide are available for large areas of the Earth, allowing for the potential investigation of active landslides in different geographic, physiographic, and climatic regions, and particularly in the many landslide areas where long-term, ground-based or sub-surface measurements are not available. The length of the deformation time series obtained by processing the ERS-1/2 and ENVISAT data is of primary importance for understanding the long-term kinematical behaviour of a landslide (Angeli et al., 2000; Malet et al., 2002; Peyret et al., 2008), and for determining the relationship (or the lack of a relationship) between the landslide history of deformation and the precipitation record (e.g., Ardizzone et al., 2011). This is a crucial information for designing remedial works and for

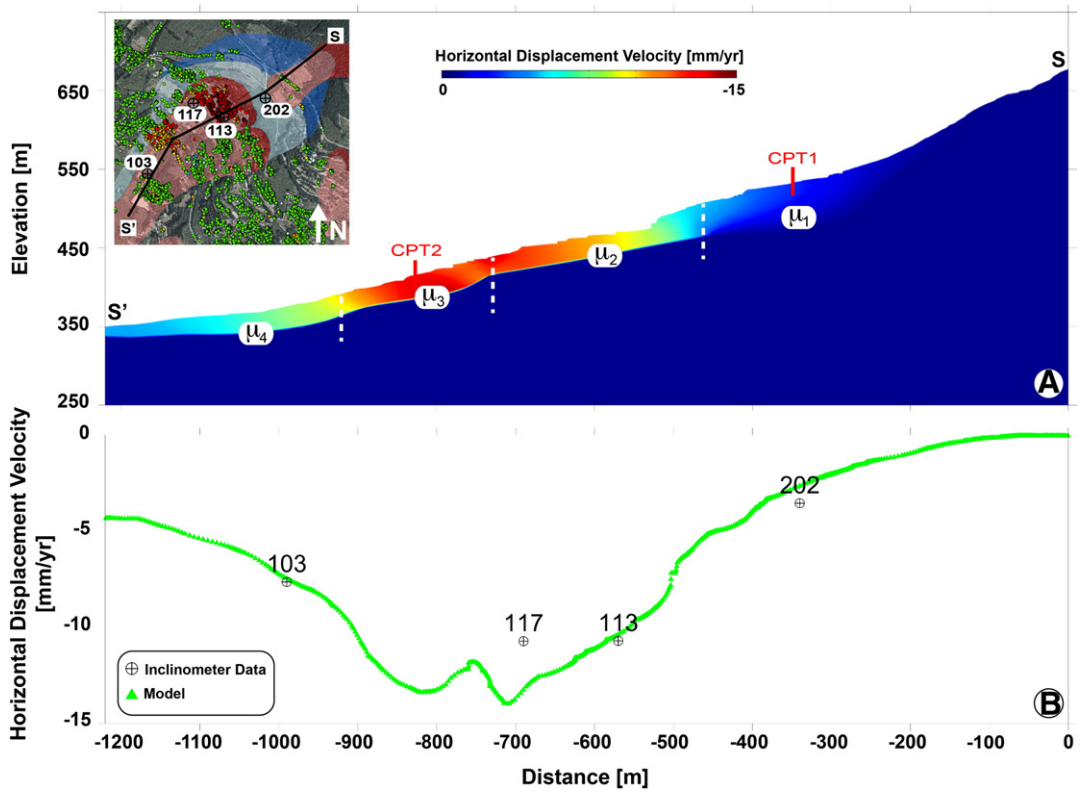


**Fig. 11.** (A) Horizontal component of the displacement field obtained from numerical modelling along the longitudinal cross section S–S' of the Ivancich landslide. CPT1 and CPT2 indicate direction changes of the profile trace. Inset shows the modelled longitudinal cross section S–S' and the location of the inclinometer boreholes, superimposed on the full resolution, ground deformation velocity map obtained processing the COSMO-SkyMed data. (B) Comparison between the horizontal component of the modelled velocity profile (green triangles) and the inclinometer data (black circles) along the longitudinal cross section of the landslide.

deciding on mitigation strategies. The possibility of preparing long time series of deformation for many landslides in different physiographic and climatic regions of the World opens to the possibility of understanding the complex, and largely unknown, relationships between climate and its variations, and the initiation and activity of deep-seated landslides (Crozier, 2010).

Next, our experiment has shown the improved capability of the new, high-resolution SAR data captured by the X-band CSK satellite sensors for landslide detection and monitoring. The significantly improved ground resolution of the CSK data (3 m × 3 m) allowed generating ground deformation velocity maps (Fig. 6A) with a 15-fold increase in the number of detected coherent points, compared to the density of points obtained using the ERS-1/2 and ENVISAT data (Fig. 6B). Although the density of points depends on many factors, including the length of the observation period (the longer the period, the lower the density of scatter points), availability of a very large number of coherent points is of the greatest importance for landslide studies. In the Ivancich landslide area, due to the large density of CSK coherent points, it was possible to: (i) detect and map the active portion of the landslide with unprecedented geographical accuracy, and (ii) to outline accurately the zones of the active landslide characterised by different mean velocities, including a narrow band of deformation along the NW boundary of the landslide, which was not visible in the ERS-1/2 and ENVISAT data. This opens to the possibility of accurate, regional scale assessments of the state of activity of landslides, in urban and sub-urban areas. The high density of CSK coherent points also allowed detecting intra-building and between-building differential settlements (Fig. 7), that can be particularly dangerous for the structural integrity and the stability of structures and infrastructures. This capability of the X-band, CSK data contributes to produce accurate landslide vulnerability and damage maps in active landslide areas. This result was difficult, or impossible, to obtain using the C-band, ERS-1/2 and ENVISAT data.

Next, we attempted an innovative use of the high-resolution DInSAR measurements obtained by processing the CSK data, in conjunction with independent thematic sub-surface information and geotechnical data, for the numerical modelling of the Ivancich active landslide (Figs. 10, 11). This represents a new frontier in landslide studies aided by remote sensing data and technologies (Bovenga et al., 2013; Guzzetti et al., 2012; Holbling et al., 2012). Despite the simplicity of the adopted physical approach, the modelling experiment produced a coherent picture of the deformation field for the Ivancich landslide area (Figs. 10, 11), with the modelled velocity in good agreement with the measurements recorded by inclinometers installed in the landslide area (Fig. 11). We maintain this is a significant advancement in the use of DInSAR products.

Finally, we consider the experiment conducted in the Ivancich landslide area as a prototype example of the application of multi-frequency SAR data for advanced landslide investigations, where the C-band, ERS-1/2 and ENVISAT data are used to produce very long time series of deformations, and the X-band, CSK data are used to prepare spatially-dense maps of the ground deformation velocity. The combined use of the different SBAS-DInSAR products maximises the advantages of the different data sets, i.e., the long-term series of displacement to understand the temporal behaviour of the slope, and the spatially-dense deformation maps for accurate activity mapping, as well as for accurate vulnerability and damage assessment in active landslide areas.

## 7. Conclusions

We used the advanced SBAS-DInSAR technique (Berardino et al., 2002; Lanari et al., 2004) to extensively investigate a deep-seated, slow-moving active landslide that affects the Ivancich residential neighbourhood, in the Assisi municipality, Central Italy (Fig. 1). Exploiting the multi-sensor capabilities of the advanced SBAS-DInSAR technique

(Bonano et al., 2012; Pepe et al., 2005), we jointly processed ERS-1/2 and ENVISAT C-band images, and we obtained deformation velocity maps for an unprecedented period of 18.6 years (Fig. 4), significantly longer than previously available for the same area (Bovenga et al., 2013; Guzzetti et al., 2009). Analysis of the DInSAR time series revealed a quasi-linear rate of displacement for the Ivancich landslide in the long observation period. The result has local and general implications. Locally, it is important for the understanding of the long-term kinematical behaviour of the active landslide, and for the design of effective remedial works. At the global scale, the possibility of preparing very long time series of deformation for landslides in different climatic regions opens to the possibility of improving our currently limited understanding of the relationships between meteorological triggers, climate variations, and the activity of deep-seated landslides (Ardizzone et al., 2011; Crozier, 2010).

Application of the SBAS-DInSAR technique to the COSMO-SkyMed X-band images allowed producing deformation velocity maps for the Ivancich landslide area with an unparalleled number of SAR coherent points, corresponding to a density of about 15,000 scatter points/km$^2$, a 15-time spatial density increase compared to the ERS-1/2 and ENVISAT data (Fig. 6). This extremely high density of measure points allowed to identify and accurately locating sections of the landslide that were more active than others, including a narrow band of deformation along the NW boundary of the landslide, and variations in the deformation velocity between buildings and within individual buildings. This result opens to the possibility of mapping landslide activity in urban areas with unprecedented accuracy, and to the production of landslide vulnerability and damage maps in active landslide areas (Galli & Guzzetti, 2007). The result is also important to support the design of landslide remedial measurements, and to monitor their efficacy.

The results of the SBAS-DInSAR processing, in conjunction with topographic, geologic and geotechnical data, including inclinometer measurements in different boreholes, were used to construct a simplified numerical model of the active landslide. The model allowed obtaining a coherent, two-dimensional picture of the landslide deformation field that is in good agreement with deep inclinometric measurements in the landslide deposit. Based on the obtained results, we foresee the possibility of using the spatially dense SBAS-DInSAR measurements for the calibration and the validation of more sophisticated numerical models of complex active landslides.

We conclude that the combined use of multiple SBAS-DInSAR products generated at different spatial and temporal scales, maximises the advantages of the different data sets, permitting an improved understanding of the long-term kinematical behaviour of the slope failure, and allowing for an accurate mapping of a landslide activity, as well as for vulnerability and damage assessment in active landslide areas.

## Acknowledgements

The work was conducted in the framework of the EC FP7 DORIS project (contract n. 242212). F. Calò, R. Castaldo, and P. Tizzani were supported by a grant of the DORIS project. We are grateful to the three anonymous reviewers, whose comments improved the quality and readability of the paper.

## References

Angeli, M. -G., Pasuto, A., & Silvano, S. (2000). A critical review of landslide monitoring experiences. *Engineering Geology*, *55*, 133–147.

Angeli, M. -G., & Pontoni, F. (2000). *The innovative use of a large diameter microtunneling technique for the deep drainage of a great landslide in an inhabited area: The case of Assisi (Italy)*. Landslides in research, theory and practice. London: Thomas Telford Publisher, 1666–1672.

Antonini, G., Ardizzone, F., Cacciano, M., Cardinali, M., Castellani, M., Galli, et al. (2002). Rapporto Conclusivo Protocollo d'Intesa fra la Regione dell'Umbria, Direzione Politiche Territoriali Ambiente e Infrastrutture, ed il CNR-IRPI di Perugia per l'acquisizione di nuove informazioni sui fenomeni franosi nella regione dell'Umbria, la realizzazione di una nuova carta inventario dei movimenti franosi e dei siti colpiti da dissesto, l'individuazione e la perimetrazione delle aree a rischio da frana di particolare rilevanza, e l'aggiornamento delle stime sull'incidenza dei fenomeni di dissesto sul tessuto insediativo, infrastrutturale e produttivo regionale. Unpublished Project Report, May 2002, 140 p. (in Italian).

Ardizzone, F., Rossi, M., Calò, F., Paglia, L., Manunta, M., Mondini, A.C., et al. (2011). Preliminary analysis of a correlation between ground deformations and rainfall: The Ivancich landslide, Central Italy. *Proceedings SPIE, Vol. 8179*, 81790L. http://dx.doi.org/10.1117/12.899453 (© 2011 SPIE CCC code: 0277-786X/11/$18).

Bell, J. W., Amelung, F., Ferretti, A., Bianchi, M., & Novali, F. (2008). Permanent scatterer InSAR reveals seasonal and long-term aquifer-system response to groundwater pumping and artificial recharge. *Water Resources Research*, *44*, W02407. http://dx.doi.org/10.1029/2007WR006152.

Berardino, P., Fornaro, G., Lanari, R., & Sansosti, E. (2002). A new algorithm for surface deformation monitoring based on small baseline differential SAR interferograms. *IEEE Transactions on Geoscience and Remote Sensing*, *40*(11), 2375–2383.

Bonano, M., Manunta, M., Marsella, M., & Lanari, R. (2012). Long term ERS/ENVISAT deformation time-series generation at full spatial resolution via the extended sbas technique. *International Journal of Remote Sensing*, *33*(15), 4756–4783. http://dx.doi.org/10.1080/01431161.2011.638340.

Bonano, M., Manunta, M., Pepe, A., Paglia, L., & Lanari, R. (2013). From previous C-band to new X-band SAR systems: Assessment of the DInSAR mapping improvement for deformation time-series retrieval in urban areas. *IEEE Transactions on Geoscience and Remote Sensing*. http://dx.doi.org/10.1109/TGRS.2012.2232933.

Borgia, A., Tizzani, P., Solaro, G., Manzo, M., Casu, F., Luongo, G., et al. (2005). Volcanic spreading of Vesuvius, a new paradigm for interpreting its volcanic activity. *Geophysical Research Letters*, *32*, L03303.

Bovenga, F., Nitti, D. O., Fornaro, G., Radicioni, F., Stoppini, A., & Brigante, R. (2013). Using C/X-band SAR interferometry and GNSS measurements for the Assisi landslide analysis. *International Journal of Remote Sensing*, *34*(11), 4083–4104. http://dx.doi.org/10.1080/01431161.2013.772310.

Bovenga, F., Wasowski, J., Nitti, D. O., Nutricato, R., & Chiaradia, M. T. (2012). Using COSMO/SkyMed X-band and ENVISAT C-band SAR interferometry for landslides analysis. *Remote Sensing of Environment*, *119*(C), 272–285. http://dx.doi.org/10.1016/j.rse.2011.12.013.

Brabb, E. E., & Harrod, B.L. (Eds.). (1989). *Landslides: Extent and economic significance*. Rotterdam: A.A. Balkema Publisher (385 pp.).

Calò, F., Calcaterra, D., Iodice, A., Parise, M., & Ramondini, M. (2012). Assessing the activity of a large landslide in southern Italy by ground-monitoring and SAR interferometric techniques. *International Journal of Remote Sensing*, *33*(11), 3512–3530.

Canuti, P., Marcucci, E., Trastulli, S., Ventura, P., & Vincenti, G. (1986). Studi per la stabilizzazione della frana di Assisi. *National Geotechnical Congress, Bologna, 14–16 May 1986, Vol. 1*. (pp. 165–174).

Cardinali, M., Antonini, G., Reichenbach, P., Guzzetti, F. (2001).Photo-geological and landslide inventory map for the Upper Tiber River basin. CNR, Gruppo Nazionale per la Difesa dalle Catastrofi Idrogeologiche, Publication n. 2154, scale 1:100,000.

Cascini, L., Fornaro, G., & Peduto, D. (2009). Analysis at medium scale of low-resolution DInSAR data in slow-moving landslide-affected areas. *ISPRS Journal of Photogrammetry and Remote Sensing*, *64*, 598–611. http://dx.doi.org/10.1016/j.isprsjprs.2009.05.003.

Cascini, L., Fornaro, G., & Peduto, D. (2010). Advanced low- and full-resolution DInSAR map generation for slow-moving landslide analysis at different scales. *Engineering Geology*, *112*(1–4), 29–42. http://dx.doi.org/10.1016/j.enggeo.2010.01.003.

Casu, F., Manzo, M., & Lanari, R. (2006). A quantitative assessment of the SBAS algorithm performance for surface deformation retrieval from DInSAR data. *Remote Sensing of Environment*, *102*, 195–210.

Corominas, J., Moya, J., Ledesma, A., Lloret, A., & Gili, J. A. (2005). Prediction of ground displacements and velocities from groundwater level changes at the Vallcebre landslide (Eastern Pyrenees, Spain). *Landslides*, *2*, 83–96.

Corsini, A., Pasuto, A., Soldati, M., & Zannoni, A. (2005). Field monitoring of the Corvara landslide (Dolomites, Italy) and its relevance for hazard assessment. *Geomorphology*, *66*, 149–165.

Covello, F., Battazza, F., Coletta, A., Lopinto, E., Fiorentino, C., Pietranera, L., et al. (2010). COSMO-SkyMed an existing opportunity for observing the Earth. *Journal of Geodynamics*, *49*(3–4), 171–180. http://dx.doi.org/10.1016/j.jog.2010.01.001.

Crozier, M. J. (2010). Deciphering the effect of climate change on landslide activity: A review. *Geomorphology*, *124*(3–4), 260–267. http://dx.doi.org/10.1016/j.geomorph.2010.04.009.

Dixon, T. H., Amelung, F., Ferretti, A., Novali, F., Rocca, F., Dokka, R., et al. (2006). Space geodesy: Subsidence and flooding in New Orleans. *Nature*, *441*, 587–588. http://dx.doi.org/10.1038/441587a.

Fastellini, G., Radicioni, F., & Stoppini, A. (2011). The Assisi landslide monitoring: A multi-year activity based on geomatic techniques. *Applied Geomatics*, *3*(2), 91–100. http://dx.doi.org/10.1007/s12518-010-0042-9.

Felicioni, G., Martini, E., & Ribaldi, C. (1996). *Studio dei Centri Abitati Instabili in Umbria*. Rubettino Publisher (418 pp., in Italian).

Ferretti, A., Prati, C., & Rocca, F. (2000). Non-linear subsidence rate estimation using permanent scatterers in differential SAR interferometry. *IEEE Transaction on Geoscience and Remote Sensing*, *38*, 2202–2212.

Ferretti, A., Prati, C., & Rocca, F. (2001). Permanent scatterers in SAR interferometry. *IEEE Transactions on Geoscience and Remote Sensing*, *39*(1), 8–20. http://dx.doi.org/10.1109/36.898661.

Galli, M., & Guzzetti, F. (2007). Landslide vulnerability criteria: A case study from Umbria, Central Italy. *Environmental Management*, *40*(4), 649–665.

Garcia-Davalillo, J. C., Herrera, G., Notti, D., Strozzi, T., & Alvarez-Fernandez, I. (2013). DinSAR analysis of ALOS PALSAR images for the assesment of very slow landslides: The Tena Valley case study. *Landslides*. http://dx.doi.org/10.1007/s10346-012-0379-8.

Giordan, D., Allasia, P., Manconi, A., Baldo, M., Santangelo, M., Cardinali, M., et al. (2013). Morphological and kinematic evolution of a large earthflow: The Montaguto landslide, southern Italy. *Geomorphology*, *187*, 61–79. http://dx.doi.org/10.1016/j.geomorph.2012.12.035.

Glade, T., Anderson, M. G., & Crozier, M. J. (Eds.). (2005). *Landslide hazard and risk*. Chichester: Wiley.

Guzzetti, F., Manunta, M., Ardizzone, F., Pepe, A., Cardinali, M., Zeni, G., et al. (2009). Analysis of ground deformation detected using the SBAS-DInSAR technique in Umbria, Central Italy. *Pure and Applied Geophysics*, *166*, 1425–1459. http://dx.doi.org/10.1007/s00024-009-0491-4.

Guzzetti, F., Mondini, A.C., Cardinali, M., Fiorucci, F., Santangelo, M., & Chang, K. -T. (2012). Landslide inventory maps: New tools for an old problem. *Earth Science Reviews*, *112*(1–2), 1–25. http://dx.doi.org/10.1016/j.earscirev.2012.02.001.

Guzzetti, F., Reichenbach, P., Cardinali, M., Galli, M., & Ardizzone, F. (2005). Probabilistic landslide hazard assessment at the basin scale. *Geomorphology*, *72*(1-4), 272–299. http://dx.doi.org/10.1016/j.geomorph.2005.06.002.

Hergarten, S., & Neugebauer, H. J. (1998). Self-organized criticality in a landslide model. *Geophysical Research Letters*, *25*(6), 801–804.

Hilley, G., Bürgmann, R., Ferretti, A., Novali, F., & Rocca, F. (2004). Dynamics of slow-moving landslides from permanent scatterer analysis. *Science*, *304*, 1952–1955. http://dx.doi.org/10.1126/science.1098821.

Holbling, D., Fureder, P., Antolini, F., Cigna, F., Casagli, N., & Lang, S. (2012). A semi-automated object-based approach for landslide detection validated by persistent scatterer inter-ferometry measures and landslide inventories. *Remote Sensing*, *4*, 1310–1336.

Hooper, A. (2008). A multi-temporal InSAR method incorporating both persistent scatterer and small baseline approaches. *Geophysical Research Letters*, *35*(16), L16302. http://dx.doi.org/10.1029/2008GL034654.

Iglesias, R., Monells, D., Centolanza, G., Mallorqui, J. J., Fabregas, X., Aguasca, A., et al. (2012). Application of high resolution spotlight TerraSAR-X data to landslide monitoring. *EUSAR, 9th European Conference on Synthetic Aperture Radar* (pp. 669–672).

Lanari, R., Berardino, P., Bonano, M., Casu, F., Manconi, A., Manunta, M., et al. (2010). Surface displacements associated with the L'Aquila 2009 Mw6.3 earthquake (Central Italy): New evidence from SBAS-DInSAR time series analysis. *Geophysical Research Letters*, *37*, L20309. http://dx.doi.org/10.1029/2010GL044780.

Lanari, R., Casu, F., Manzo, M., Zeni, G., Berardino, P., Manunta, M., et al. (2007). An overview of the Small BAseline Subset algorithm: A DInSAR Technique for surface deformation analysis. *Pure and Applied Geophysics*, *164*, 647–661. http://dx.doi.org/10.1007/s00024-007-0192-9.

Lanari, R., Mora, O., Manunta, M., Mallorqui, J., Berardino, P., & Sansosti, E. (2004). A small baseline approach for investigating deformations on full resolution differential SAR interferograms. *IEEE Transactions on Geoscience and Remote Sensing*, *42*, 1377–1386.

Malet, J. -P., Maquaire, O., & Calais, E. (2002). The use of global positioning system techniques for the continuous monitoring of landslides: Application to the Super-Sauze earthflow (Alpes-de-Haute-Provence, France). *Geomorphology*, *43*, 33–54.

Manconi, A., Walter, T. R., Manzo, M., Zeni, G., Tizzani, P., Sansosti, E., et al. (2010). On the effects of 3-D mechanical heterogeneities at Campi Flegrei caldera, southern Italy. *Journal of Geophysical Research*, *115*, B08405. http://dx.doi.org/10.1029/2009JB007099.

Manunta, M., Marsella, M., Zeni, G., Sciotti, M., Atzori, S., & Lanari, R. (2008). Two-scale surface deformation analysis using the SBAS-DInSAR technique: A case study of the city of Rome, Italy. *International Journal of Remote Sensing*, *29*(6), 1665–1684.

Massonnet, D., Briole, P., & Arnaud, A. (1995). Deflation of Mount Etna monitored by spaceborne radar interferometry. *Nature*, *375*, 567–570.

Massonnet, D., Rossi, M., Carmona, C., Ardagna, F., Peltzer, G., Feigl, K., et al. (1993). The displacement field of the Landers earthquake mapped by radar interferometry. *Nature*, *364*, 138–142.

Mora, O., Mallorqui, J. J., & Broquetas, A. (2003). Linear and nonlinear terrain deformation maps from a reduced set of interferometric SAR images. *IEEE Transactions on Geoscience and Remote Sensing*, *41*(10), 2243–2253. http://dx.doi.org/10.1109/TGRS.2003.814657.

Pepe, A., Sansosti, E., Berardino, P., & Lanari, R. (2005). On the generation of ERS/ENVISAT DInSAR time-series via the SBAS technique. *IEEE Geosciences and Remote Sensing Letters*, *2*(3), 265–269.

Petley, D. (2012). Global patterns of loss of life from landslides. *Geology*, *40*(10), 927–930.

Petley, D. N., Mantovani, F., Bulmer, M. H., & Zannoni, A. (2005). The use of surface monitoring data for the interpretation of landslide movement patterns. *Geomorphology*, *66*, 133–147.

Peyret, M., Djamour, Y., Rizza, M., Ritz, J. -F., Hurtrez, J. -E., Goudarzi, M.A., et al. (2008). Monitoring of the large slow Kahrod landslide in Alborz mountain range (Iran) by GPS and SAR interferometry. *Engineering Geology*, *100*, 131–141.

Pontoni, F. (1999). Unpublished Technical Report, 45 pp., July 1999 (in Italian).

Pontoni, F. (2011). Geoequipe Studio Tecnico Associato Geologia – Ingegneria. Unpublished Technical Report, 4 pp., May 2011 (in Italian).

Reichenbach, P., Galli, M., Cardinali, M., Guzzetti, F., & Ardizzone, F. (2005). Geomorphological mapping to assess landslide risks: Concepts, methods and applications in the Umbria region of Central Italy. In T. W. Glade, M. G. Anderson, & M. J. Crozier (Eds.), *Landslide hazard and risk* (pp. 429–468). John Wiley & Sons.

Revellino, P., Grelle, G., Donnerumma, A., & Guadagno, F. M. (2010). Structurally controlled earth flows of the Benevento province (southern Italy). *Bulletin of Engineering Geology and the Environment*, *69*, 487–500.

Rossi, M., Witt, A., Guzzetti, F., Malamud, B.D., & Peruccacci, S. (2010). Analysis of historical landslide time series in the Emilia–Romagna region, northern Italy. *Earth Surface Processes and Landforms*, *35*, 1123–1137. http://dx.doi.org/10.1002/esp.1858.

Servizio Geologico Italiano (1980). Carta Geologica dell'Umbria. Map at 1:250,000 scale, (in Italian).

Tizzani, P., Manconi, A., Zeni, G., Pepe, A., Manzo, M., Camacho, A., et al. (2010). Long-term versus short-term deformation processes at Tenerife (Canary Islands). *Journal of Geophysical Research*, *115*, B12412. http://dx.doi.org/10.1029/2010JB007735.

Tommasi, P., Pellegrini, P., Boldini, D., & Ribacchi, R. (2006). Influence of rainfall regime on hydraulic regime and movement rates in the overconsolidated clayey slope of the Orvieto hill (Central Italy). *Canadian Geotechnical Journal*, *43*, 70–86.

Van Westen, C. J., Van Asch, T. W. J., & Soeters, R. (2006). Landslide hazard and risk zonation — why is it still so difficult? *Bulletin of Engineering Geology and Environment*, *65*, 167–184.

Werner, C., Wegmuller, U., Strozzi, T., & Wiesmann, A. (2003). Interferometric point target analysis for deformation mapping. *2003 IEEE International Geoscience and Remote Sensing Symposium* (pp. 4362–4364). France: Toulose.

Witt, A., Malamud, B. D., Rossi, M., Guzzetti, F., & Peruccacci, S. (2010). Temporal correlations and clustering of landslides. *Earth Surface Processes and Landforms*, *35*(10), 1138–1156. http://dx.doi.org/10.1002/esp.1998.